Available online at www.sciencedirect.com

ScienceDirect

Procedia CIRP 31 (2015) 124 – 129

www.elsevier.com/locate/procedia

15th CIRP Conference on Modelling of Machining Operations

Finite element prediction of the tool wear influence in Ti6Al4V machining

François Ducobu[a,*], Pedro-José Arrazola[b], Edouard Rivière-Lorphèvre[a], Enrico Filippi[a]

[a] *University of Mons (UMONS), Faculty of Engineering (FPMs), Machine Design and Production Engineering Department, 20 Place du Parc, B-7000 Mons, Belgium*

[b] *Mondragon University, Faculty of Engineering, Mechanical and Manufacturing Department, Mondragón 20500, Spain*

[*] Corresponding author. Tel.: +32-65-45-47; fax: +32-65-45-45. *E-mail address:* Francois.Ducobu@umons.ac.be

Abstract

Ti6Al4V is a titanium alloy widely used in the aeronautical industry and machining is often adopted to manufacture it. These parts must satisfy requirements specified by the customer. A crucial characteristic of aircraft machined parts is their reliability and, therefore, their fatigue life has to be mastered. In this context, the corresponding requirement concerns the surface integrity. This should be achieved by selecting adequate cutting parameters, which is actually not an immediate operation. The geometry of the tool will afterwards change during its life, what is more as Ti6Al4V is known to be a hard-to-machine material. In this context, a finite element model is developed to highlight the influence of tool wear on fundamental variables like forces, temperatures, stresses,... and surface integrity (through plastic strains). The results should help to decide when it is time to replace the tool before altering the part and therefore not meet the specifications anymore.

Peer-review under responsibility of the International Scientific Committee of the "15th Conference on Modelling of Machining Operations

Keywords: Surface integrity, Titanium, Finite element method (FEM)

1. Introduction

The quality of the surface obtained by machining is influenced by many parameters: the cutting conditions, the microstructure of the material and its potential evolution due to the machining, the tool angles and wear. The quality of the machined surface can be specified on a technical drawing through the imposition of a maximal arithmetic roughness value. This can be required to lead to a good compatibility in an assembly if the surfaces are in contact, to allow a following surface treatment (coating for example), but this is also related to the fatigue strength of the material. Fatigue life, resistance against fracture, and therefore the reliability of the part, wear and corrosion depends on the surface integrity as well [1].

In the aeronautical industry, the reliability of a part is an important requirement. Fatigue life has a direct influence on it and should therefore be mastered. An increasing number of components is made of Ti6Al4V, a titanium alloy known to have good mechanical properties for a low density, but also to be a hard-to-machine material. Controlling the surface integrity due to machining is still a challenge nowadays. While the cutting conditions and the proper tool selection is a step that, although being still time consuming and expensive, can be achieve through an experimental campaign, the influence of the tool wear on the microstructure and on the surface integrity is still an ongoing problem. The evolution of the tool geometry with the increase of wear makes it even more difficult. When should the tool be replaced before damaging the surface but without not fully using it is not an easy question to answer.

The numerical prediction of the residual stresses is still difficult, mainly due to the properties of the machined material to introduce in the model and their effects on plastic deformation, chip formation, separation, and fracture, according to Jawahir et al. [2]. Torrano et al. [3] shows via a benchmark study the significant differences in the residual stresses profiles, depending on the code and the material adopted. The geometry of the tool is a parameter that also should not be neglected. The effects of the tool wear on the residual stresses during Ti6Al4V orthogonal cutting were investigated by Chen et al. [4] with a finite element model. Sasahara et al. [5] studied the influence of the cutting parameters and tool geometry on the residual stresses and Özel and Ulutan [6] performed a Ti6Al4V residual stresses prediction in a 3D finite element model. The worn tool geometry has to be known as an input in these models. The prediction of the tool wear in terms of flank wear, as well as crater wear is another difficult topic because of the multiple mechanisms and parameters it involves. Schulze et al. [7] predicted the flank wear in orthogonal cutting of Ti6Al4V with a finite element model. Some, as Xie et al. [8], Filice et al. [9] or Attanasio et al. [10,11], developed numerical models in which the geometry of the tool is updated to take account of the wear. The procedures and computation of these models seem rather heavy.

Peer-review under responsibility of the International Scientific Committee of the "15th Conference on Modelling of Machining Operations
doi:10.1016/j.procir.2015.03.056

In [12] and for Inconel 718, Arrazola et al. study experimentally the influence of flank wear on cutting forces, the roughness and the surface integrity of the machined surface. They show that tool wear could be monitored directly from signals of the CNC controller of the lathe. This experimental study demonstrates the link between tool wear, cutting forces and machined surface and has no numerical equivalent so far, to the author's knowledge.

Following these experimental observations, this paper is a first numerical step to study the influence of the tool wear in Ti6Al4V machining, focusing on flank wear with a non-adaptive tool geometry and a "classical" constitutive law. It intends to highlight the influence of tool wear on fundamental variables like forces, temperatures, stresses,... and surface integrity with a finite element model in Ti6Al4V orthogonal cutting. In this paper, only plastic strain is taken into account when considering the surface integrity. Although not being carried out on the same material, the experiments of Arrazola et al. [12] should give the general experimental trends.

2. Presentation of the finite element model

2.1. Common features

In order to study the influence of the tool wear on the Ti6Al4V chip formation, a thermomechanical numerical model has been developed with the commercial finite element software ABAQUS/Explicit v6.11. It consists of a 2D plane strain orthogonal cutting model and takes into account the area close to the cutting edge of the tool. In this model, the tool is fixed in space and the workpiece material "flows" around the cutting edge radius (Fig. 1).

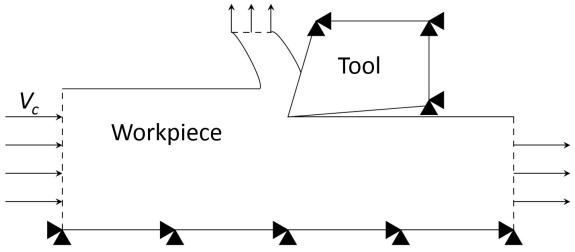

Fig. 1. Schematical representation and boundary conditions of the model.

The mechanical formulation adopted for the workpiece is the Arbitrary Lagrangian Eulerian (ALE) formulation, which combines the features of pure Lagrangian and Eulerian analysis, with Eulerian boundaries Özel and Zeren [13]. In the ALE formulation, the mesh is not attached to the material and can move to avoid distortions and to update the free chip geometry. The chip formation is simulated via adaptive meshing and plastic flow of the workpiece material. This implies that there is no chip separation criterion in the proposed model. The workpiece can be seen as a pipe into which the material flows. The entrance (left face of the workpiece) and the exits (the right face of the workpiece and the upper face of the chip) are modelled as Eulerian boundaries, allowing material to flow through them. All other surfaces are modelled as "classical" Lagrangian boundaries. The shape of the bottom surface of the workpiece is fixed while the shape of the upper surface is free to deform. The tool and workpiece meshes range, respectively, approximately from 250 to 360 and from 2600 to 3700 four-node elements, depending on the tool geometry. The meshes are refined in the close area around the tool edge radius.

Table 1. Material properties, cutting conditions and tool geometries [14–16].

Johnson-Cook law	A (*MPa*)	862
	B (*MPa*)	331
	C	0.012
	m	0.8
	n	0.34
Inelastic heat fraction	Ti6Al4V	0.9
Density (kg/m^3)	Ti6Al4V	4430
	Carbide	15,000
Young's modulus (*GPa*)	Ti6Al4V	113.8
	Carbide	800
Expansion (K^{-1})	Ti6Al4V	8.6
	Carbide	4.7
Conductivity (*W/mK*)	Ti6Al4V	7.3
	Carbide	46
Specific heat (*J/KgK*)	Ti6Al4V	580
	Carbide	203
Friction coefficient		0.3
Friction energy to heat		1
Thermal conductance (W/m^2K)		1,000,000
Heat partition coefficient		0.5
Cutting speed (*m/min*)		80
Depth of cut (*mm*)		0.1
Width of cut (*mm*)		1
Rake angle (°)		7
Clearance angle (°)		6
Cutting edge radius (μm)		20
Flank wear length (*mm*)	0-01	0.1
	0-03	0.3
	-3-01	0.1
	-3-03	0.3
Worn clearance angle (°)	0-01	0
	0-03	0
	-3-01	-3
	-3-03	-3

The workpiece material (Ti6Al4V) is assumed to be homogeneous and its behaviour is described by the Johnson-Cook plasticity model, while the tool is in tungsten carbide described by a linear elastic law. Friction at the tool-chip interface is implemented using a Coulombic friction law and a constant friction coefficient. It is assumed that all of the dissipated heat due to friction is converted into heat and that this heat flows equally into the chip and the tool. The initial temperature of the model is 25°C. Only conduction is considered in the present model and it is assumed that the transformation of deformation to heat efficiency is 90%. The parameters of the model are given in Table 1.

2.2. Tool geometries

The tool is modelled with a finite edge radius of 20 µm, a rake angle of 7° and a clearance angle of 6°, which are typical angles values in Ti6Al4V turning. The cutting conditions adopted are a cutting speed, V_c, of 80 m/min (typical industrial cutting speed) and a depth of cut (uncut chip thickness), h, of 0.1 mm. The length of the workpiece before the chip is equal to

3 h (0.3 mm) and the length of the workpiece after the contact with the tool is also set to 3 h (0.3 mm).

Five tool geometries are considered in this paper. The first one is the new tool (Fig. 2) with the values given previously. Different worn tool are then studied. The first type of worn tool has a clearance angle of 0° and a flank wear of 0.1 mm or 0.3 mm long (Fig. 2). The second type of worn tool has a clearance angle of -3° and a flank wear of 0.1 mm or 0.3 mm long (Fig. 2). The geometry of the real worn tool (and its evolution) being unknown, this allows to consider different potential situations, taking into account that a flank wear of 0.3 mm long is the limit value to continue to use a tool [17]. The geometries presented in Fig. 2 were selected based on observations made after experimental tests carried on in the past in cutting conditions different of that of this article. They are consequently not chosen randomly but clearly reflect expected geometries. Tendencies of the influence of the tool wear on the cut are therefore sought through this modelling.

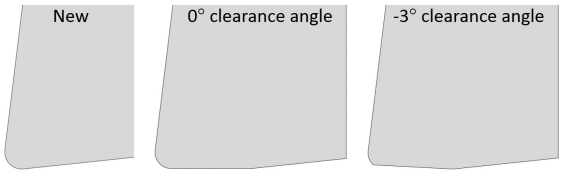

Fig. 2. Three types of tool geometries.

The tool geometry with a -3° clearance angle is considered because it could be the evolution of a 0° clearance angle geometry when the wear is increasing. It consists of a loss of material on the flank face and the edge radius (still considered as an ideal arc in this study) starting from a geometry with a 0° clearance angle, as shown in Fig. 3. The complete suppression of the edge radius is another potential worn tool geometry. This was initially considered as well but lead to numerical problems: a significant penetration of the tool in the workpiece is observed and the elements in this area are not able to flow around the tool to fit its geometry, ending in excessive (and unacceptable) elements distortion terminating the computation.

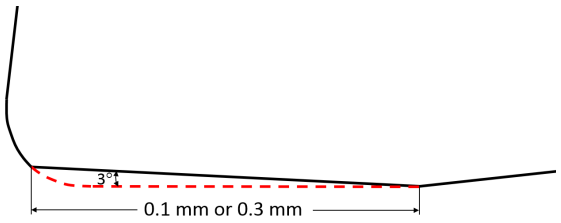

Fig. 3. Detail of the -3-0x tool geometries.

3. Results

Temperature contours are plotted in Fig. 4. With the initial tool geometry, the highest temperature is obtained in the chip, in the secondary shear zone (where the chip is in contact with the rake face of the tool). For the same wear type (0° clearance angle or -3° clearance angle), the temperature increases with the length of the flank wear. It is also noted that the -3° clearance angle leads to a higher temperature than the 0° clearance angle. The location of the maximum temperature moves with the geometry of the tool: it remains in the machined material but goes from the rake face area (secondary shear zone) to the flank face area (tertiary shear zone) when the tool wear increases. Chen et al. [4] also observed, with a numerical model, the introduction of a hot spot on the flank face of the workpiece. Like in this study, the high temperature in the tertiary shear zone appeared for high flank wear values.

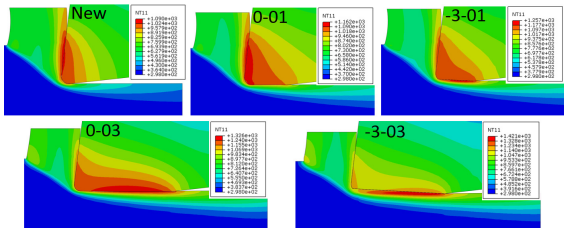

Fig. 4. Temperature contours (in K) after 3.5 ms (3 ms for -3-03), different temperature scales.

Temperatures on two particular points are plotted in Fig. 6. Both of these points are chosen on the outer surface of the workpiece (Fig. 5): the first one is at approximately 0.75 mm of the cutting edge radius in the rake face area of the chip (thus in the secondary shear zone) and the second one is at approximately 0.75 mm of the cutting edge radius in the rake face area of the machined surface (in the tertiary shear zone). Fig. 5 also shows that the mesh is virtually not deformed in the three shear zones, allowing to be confident in the numerical results and the choice of the adopted numerical formulation.

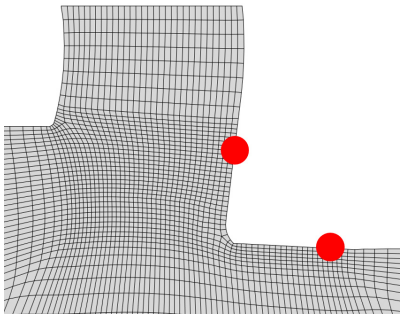

Fig. 5. Location of the two points where temperature is studied.

As expected, the temperature is higher in the secondary shear zone than in the tertiary one for the initial tool geometry. The temperature of the point near the rake face increases slightly with the tool wear. Near the rake face, on the contrary, the temperature increase is much larger and the temperature in that area becomes larger than in the secondary shear zone. This is consistent with the temperature contours of Fig. 4. The general trend of the temperature of the first point (secondary shear zone) remains the same when the tool geometry changes. For the second point (tertiary shear zone), differences are observed. With a clearance angle of 0°, a larger increase occurs (a kind

Table 2. Mean temperatures (between 3.5 ms and 5 ms, 1.5 ms and 3 ms for -3-03) in the secondary and tertiary shear zones.

	New	0-01	0-03	-3-01	-3-03
Rake face (*K*)	1108	1168	1168	1197	1122
Flank face (*K*)	595	965	1276	1277	1182
$\frac{\text{Flank face}}{\text{Rake face}}$	0.54	0.83	1.09	1.07	1.05

Table 3. RMS of the cutting forces (between 3.5 ms and 5 ms, 1.5 ms and 3 ms for -3-03).

	New	0-01	0-03	-3-01	-3-03
Cutting force (*N/mm*)	149	165	227	179	243
Feed force (*N/mm*)	60	119	385	190	464
$\frac{\text{Cutting force}}{\text{Feed force}}$	0.41	0.72	1.70	1.06	1.91

of step in the temperature) after a time larger for a longer flank wear. With a clearance angle of -3°, the temperature evolution is similar to that in the first point for the short flank wear (-3-01), while small fluctuations at high frequency are noted for the longer flank wear (-3-03). During the chip formation of that last case (-3-03), oscillations on the free surface of the chip, in the primary shear zone, were noted, indicating that the chip is certainly not continuous any more but has a kind of small teeth. These oscillations lead to the premature termination of the computing (shortly after 3 ms of simulation time) due to excessive element distortion on the free surface of the chip, in the primary shear zone. The mean values of the temperatures are given in Table 2. They confirm the tendencies observed in Fig. 6. The temperatures for the -3-03 tool geometry are lower due to the smaller simulation time at which they are computed. The numerical values clearly show the large increase of the temperature in the tertiary shear zone due to the tool wear.

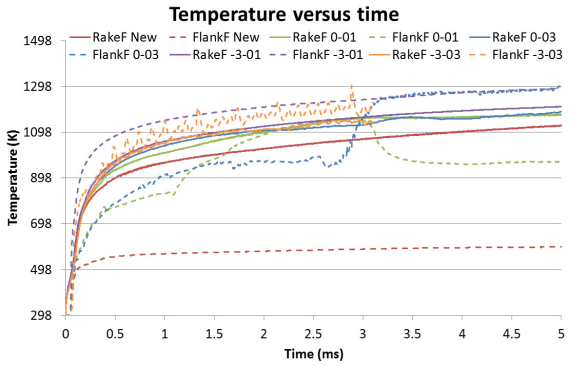

Fig. 6. Temperature evolutions on two points of the rake face (RakeF) and the flank face (FlankF) of the workpiece.

Due to the contact of the flank face of the tool on the workpiece when it is worn, friction is larger and the cutting forces are expected to increase, and particularly the force in the vertical direction, i.e. the feed force. Fig. 7 clearly shows that the cutting forces are affected by the tool wear. The forces with the new tool geometry become quickly constant and the cutting force is larger than the feed force. With the increase of the tool wear, the cutting force increases but the feed force increases more, as shown by the ratio of the RMS of the cutting force on the RMS of the feed force in Table 3. Indeed, for the 0-03, -3-01 and -3-03 tool geometries, the feed force is larger than the cutting force and that ratio increases with the tool wear (it is higher for -3-03 than -3-01 for example). The observations about the different evolutions are similar to that of the temperatures in Fig. 6. The decrease in time of the forces (hardly noticeable in Fig. 7 for the new and -3-01 cases) is linked to the temperature evolutions: lower forces are due to the thermal softening of the workpiece material.

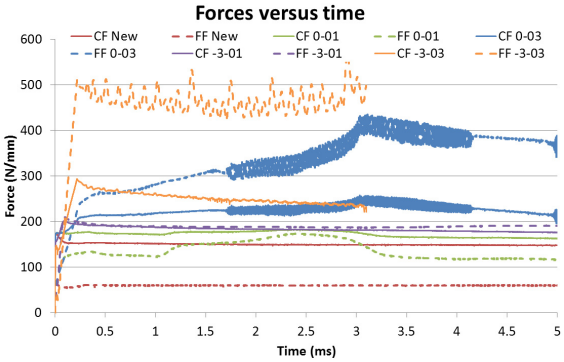

Fig. 7. Cutting forces (CF) and feed forces (FF) evolutions for the five tool geometries.

The evolution of the feed force for the -3-03 geometry confirms that the chip is certainly not continuous; it is less obvious on the cutting force evolution. Distinct evolutions are noted, depending on the value of the clearance angle. When it is 0°, the force increases with time then a step in the increase occurs and the forces decreases afterwards. With a -3° clearance angle, there is a large increase in the force in a short period of time and then it slightly decreases. The experimental study of Arrazola et al. [12] on Inconel 718 also concluded that the forces increase with the tool flank wear. This increase was sharper for a longer flank wear. Like in this study, the cutting force increase was lower than for the feed force. The obtained numerical results are therefore qualitatively in accordance with that experimental reference.

The cutting forces have been experimentally measured for a tool with 0-02 geometry (clearance angle of 0° and flank wear of 0.2 mm). This was a first test to validate the experimental setup that will be used to carry on an experimental campaign focusing on the influence and evolution of tool wear on the Ti6Al4V cutting process. The setup was close to that introduced in ref. [18]. It uses a milling machine as a planning machine to operate in strictly orthogonal cutting conditions, as in the numerical modelling. The uncut chip thickness was 0.1 mm, as in the finite element model of this paper, and the cutting speed was 30 m/min (it is the maximum feed rate of the machine). The RMS value of the cutting force is 236 N/mm, the RMS of the feed force is 288 N/mm and their ratio is 1.22. Although the cutting conditions are different, this values showed the influence of the flank wear on the cutting forces. Indeed, as for the numerical model, the feed force with a tool significantly worn was larger than the cutting force. The values cannot directly be compared to these of the modelling as the cutting speeds were different but most of them were found between

Table 4. Normalized equivalent plastic strains and frictional dissipation (between 3.5 ms and 5 ms, 1.5 ms and 3 ms for -3-03).

	0-01	0-03	-3-01	-3-03
Plastic strains	1.15	3.18	7.33	4.96
Frictional dissipation	1.92	3.75	1.36	1.83

these of the 0-01 and 0-03 geometries, which was expected. The trends given by the modelling are therefore in accordance with the experimental observations on that point.

The plastic strains at the second point (in the tertiary shear zone) are plotted for the five tool geometries in Fig. 8. Strains in the chip are not plotted as our interest is focused on the machined surface. The values in that figure are adimensional ones: they are all divided by the value obtained with the initial tool geometry to get a normalized quantity. This shows that the plastic strains increase with the tool wear and that the negative clearance angle leads to higher strains (Table 4). The worse tool geometry on that aspect is the -3-01, although it was expected that it would be the -3-03 situation due to the previous observations. Higher equivalent plastic strains at the workpiece surface suggest that the residual stresses in the workpiece will be higher and therefore decrease the quality of the machined part. When the flank wear of the tool increases, Arrazola et al. [12] observed that surface integrity defects appeared more frequently (and particularly for a flank wear length larger than 0.15 mm). The higher plastic strains obtained with the numerical model are therefore consistent with their experimental findings.

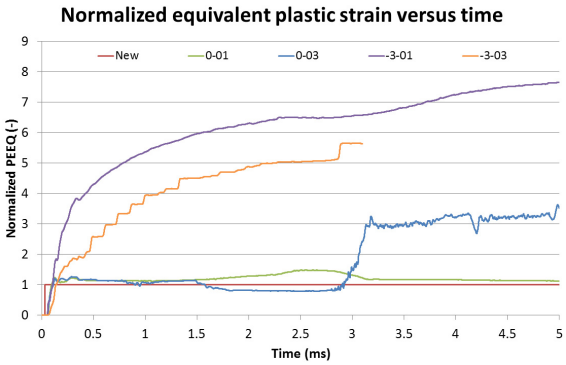

Fig. 8. Normalized equivalent plastic strains evolutions in the tertiary shear zone.

As for the normalized plastic strains, the normalized frictional dissipation, plotted in Fig. 9, consists of the current value divided by the one with the initial tool geometry. For all the tool geometries with wear, the frictional dissipation is larger than the new tool geometry (Table 4). As expected, it is larger when the clearance angle is 0°: the material flows with more difficulty against the flank face of the tool than when there is an angle. Friction is also higher when the length of the flank wear is larger as well. As for the cutting forces, two different evolutions are observed depending on the value of the clearance angle.

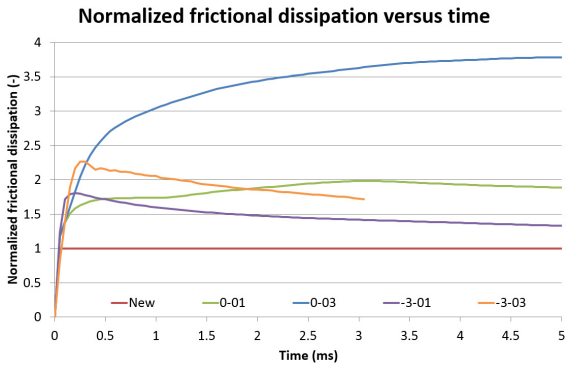

Fig. 9. Normalized frictional dissipation evolutions for the different tool geometries.

4. Conclusions and perspectives

The tool geometries with the longer flank wear (x-03) lead to values (temperatures, forces, plastic strains and frictional dissipation) much higher than in the reference case with a new tool. It is thus expected that a degradation of the surface integrity would occur for that flank wear length. When this was shorter (x-01), a negative influence of the tool wear on the results was noted as well. The tool geometry with a -3° clearance angle had by the way more influence on the results and would therefore be more harmful for the surface integrity. The combination of that angle value with the longest flank wear (-3-03) constituted the tool geometry impacting the most the machined surface. The chip formation with that tool was also modified: the chip morphology was going away from the initial continuous chip. All these results were qualitatively in accordance with the expectations and observations form the literature.

This numerical study allowed to highlight the influence of the wear (and geometry) of the tool on the chip formation and the machined surface. It showed that an experimental measure of the cutting forces should allow to detect a too much worn tool. Such a tool ends in an increase of the temperature and the plastic strains in the machined surface, which could induce modifications of the microstructure and increase the residual stresses, harmful for the reliability of the machined workpiece.

An experimental campaign in the same cutting conditions as the developed model will next be performed in order to quantitatively validate the numerical predictions. Improvements of the model to take into account the evolution of the flank wear of the tool with the increase of the cutting length (i.e. an adaptive tool geometry) should be implemented in a second time.

Acknowledgements

The authors thank the *Fonds de la Recherche Scientifique de Belgique* (FRS-FNRS), Wallonie-Bruxelles International (*Bourse d'excellence WBI.World*) and the projects InProRet (code IE12-342), InProRet II (code IE13-365) for the financial support provided for the research presented trough this paper.

References

[1] Arrazola, P., Özel, T., Umbrello, D., Davies, M., Jawahir, I.. Recent advances in modelling of metal machining processes. CIRP Annals – Manufacturing Technology 2013;62:695–718.

[2] Jawahir, I., Brinksmeier, E., M'Saoubi, R., Aspinwall, D., Outeiro, J., Meyer, D., et al. Surface integrity in material removal processes: Recent advances. CIRP Annals – Manufacturing Technology 2011;60:603–626.

[3] Torrano, I., Barbero, O., Soriano, J., Kortabarria, A., Arrazola, P.. Prediction of residual stresses in turning of inconel 718. Advanced Materials Research 2011;223:421–430.

[4] Chen, L., El-Wardany, T., Harris, W.. Modelling the effects of flank wear land and chip formation on residual stresses. CIRP Annals – Manufacturing Technology 2004;53:95–98.

[5] Sasahara, H., Obikawa, T., Shirakashi, T.. Prediction model of surface residual stress within a machined surface by combining two orthogonal plane models. International Journal of Machine Tools and Manufacture 2004;44:815–822.

[6] Özel, T., Ulutan, D.. Prediction of machining induced residual stresses in turning of titanium and nickel based alloys with experiments and finite element simulations. CIRP Annals – Manufacturing Technology 2012;61:547–550.

[7] Schulze, V., Michna, J., Zanger, F., Pabst, R.. Modeling the process-induced modifications of the microstructure of work piece surface zones in cutting processes. Advanced Materials Research 2011;223:371–380.

[8] Xie, L., Schmidt, J., Schmidt, C., Biesinger, F.. 2D FEM estimate of tool wear in turning operation. Wear 2005;258:1479–1490.

[9] Filice, L., Micari, F., Settineri, L., Umbrello, D.. Wear modelling in mild steel orthogonal cutting when using uncoated carbide tools. Wear 2007;242:545–554.

[10] Attanasio, A., Ceretti, E., Rizzuti, S., Umbrello, D., Micari, F.. 3D finite element analysis of tool wear in machining. CIRP Annals – Manufacturing Technology 2008;57:61–64.

[11] Attanasio, A., Umbrello, D.. Abrasive and diffusive tool wear FEM simulation. International Journal of material Forming 2009;2:543–546.

[12] Arrazola, P., Garay, A., Fernandez, E., Ostolaza, K.. Correlation between tool flank wear, force signals and surface integrity when turning bars of inconel 718 in finishing conditions. International Journal of Machining and Machinability of Materials 2014;15:84–100.

[13] Özel, T., Zeren, E.. Finite element modeling the influence of edge roundness on the stress and temperature fields induced by high-speed machining. International Journal of Advanced Manufacturing Technology 2007;35:255–267.

[14] Meyer, H., Kleponis, D.. Modeling the high strain rate behavior of titanium undergoing ballistic impact and penetration. International Journal of Impact Engineering 2001;26:509–521.

[15] Ducobu, F., Rivière-Lorphèvre, E., Filippi, E.. Numerical contribution to the comprehension of saw-toothed Ti6Al4V chip formation in orthogonal cutting. International Journal of Mechanical Sciences 2014;81:77 – 87. doi:10.1016/j.ijmecsci.2014.02.017.

[16] Calamaz, M., Coupard, D., Girot, F.. Numerical suimulation of titanium dry machining with a strain softening constitutive law. Machining Science and Technology 2010;14:244–257. doi:10.1080/10910344.2010.500957.

[17] 3685, I.S.I.. Tool-life testing with single point turning tools 1993;A.

[18] Ducobu, F., Rivière-Lorphèvre, E., Filippi, E.. Experimental contribution to the study of the Ti6Al4V chip formation in orthogonal cutting on a milling machine. International Journal of Material Forming 2014;doi:10.1007/s12289-014-1189-4.